REVIEW

Nano-sized manganese oxides as biomimetic catalysts for water oxidation in artificial photosynthesis: a review

Mohammad Mahdi Najafpour[1,2,*], Fahimeh Rahimi[1], Eva-Mari Aro[3], Choon-Hwan Lee[4] and Suleyman I. Allakhverdiev[5,6,*]

[1]*Department of Chemistry, and* [2]*Center of Climate Change and Global Warming, Institute for Advanced Studies in Basic Sciences* (*IASBS*), *Zanjan, Iran*
[3]*Department of Biochemistry and Food Chemistry, University of Turku, 20014 Turku, Finland*
[4]*Department of Molecular Biology, Pusan National University, Busan, 609-735, Korea*
[5]*Institute of Plant Physiology, Russian Academy of Sciences, Botanicheskaya St. 35, Moscow 127276, Russia*
[6]*Institute of Basic Biological Problems, Russian Academy of Sciences, Pushchino, Moscow Region 142290, Russia*

There has been a tremendous surge in research on the synthesis of various metal compounds aimed at simulating the water-oxidizing complex (WOC) of photosystem II (PSII). This is crucial because the water oxidation half reaction is overwhelmingly rate-limiting and needs high over-voltage (approx. 1 V), which results in low conversion efficiencies when working at current densities required for hydrogen production via water splitting. Particular attention has been given to the manganese compounds not only because manganese has been used by nature to oxidize water but also because manganese is cheap and environmentally friendly. The manganese–calcium cluster in PSII has a dimension of about approximately 0.5 nm. Thus, nano-sized manganese compounds might be good structural and functional models for the cluster. As in the nanometre-size of the synthetic models, most of the active sites are at the surface, these compounds could be more efficient catalysts than micrometre (or bigger) particles. In this paper, we focus on nano-sized manganese oxides as functional and structural models of the WOC of PSII for hydrogen production via water splitting and review nano-sized manganese oxides used in water oxidation by some research groups.
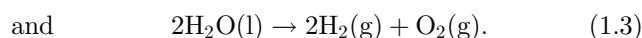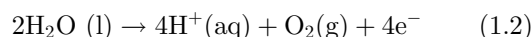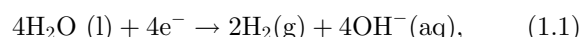
Keywords: manganese; nano-sized manganese oxides; photosystem II; water oxidation; water splitting

1. INTRODUCTION

Artificial photosynthesis is a research field that attempts to replicate the natural process of photosynthesis [1–3]. The goal of artificial photosynthesis is to use sunlight energy to make different useful materials or high-energy chemicals to store energy (scheme 1) [1–3].

Hydrogen may be an ideal fuel for the future [4–9]. Hydrogen generation by water reduction equation (1.1) in water splitting equation (1.3) has been proposed as the holy grail of chemistry [10]. In the water

splitting reaction, the water oxidation equation (1.2) involving four-electron transfer is more difficult owing to thermodynamic and kinetic limitations:

$$4H_2O\ (l) + 4e^- \rightarrow 2H_2(g) + 4OH^-(aq), \qquad (1.1)$$

$$2H_2O\ (l) \rightarrow 4H^+(aq) + O_2(g) + 4e^- \qquad (1.2)$$

and

$$2H_2O(l) \rightarrow 2H_2(g) + O_2(g). \qquad (1.3)$$

The reaction provides electrons not only for proton reduction but also for other reduction reactions that are equally important in artificial photosynthesis (scheme 1). The only system to catalyse water oxidation in nature is the water-oxidizing complex (WOC) of

*Authors for correspondence (mmnajafpour@iasbs.ac.ir; suleyman. allakhverdiev@gamil.com).
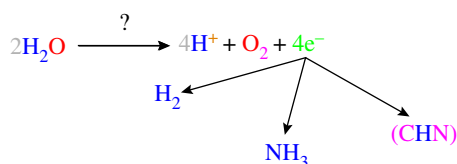
Scheme 1. During water oxidation, in addition to oxygen evolution, electrons and protons are also produced, which could be used in synthesizing fuel and useful compounds. (Online version in colour.)

photosystem II (PSII) in cyanobacteria, algae and plants (figure 1) [11–23].

The WOC is a manganese–calcium cluster housed in a protein environment of PSII that controls reaction coordinates, proton movement and water access [22,23].

The first clear image for the cubane model came from James Barber and So Iwata's groups in 2004 [16]. These groups also provided, for the first time, information on Ca in the WOC. They show that manganese–calcium is a Mn_3Ca-cubane with the fourth Mn attached further away [16].

Recently, Jian-Ren Shen and Nobuo Kamiya groups dramatically improved the resolution of the PSII crystals from the thermophilic cyanobacterium *Thermosynechococcus vulcanus* to $1.9\,\text{Å}$ and analysed their structure in detail (figure 1). They showed that the manganese–calcium cluster can be considered as $CaMn_4O_5(H_2O)_4$ [22,23].

The structure is shown in figure 1. In the structure, Mn(1) has three (μ_3-O), one monodentate carboxylate, one bridging carboxylate and one imidazole ligand [22,23]. The ligands around Mn(1) are similar to those found in manganese ions in manganese catalase enzymes [22,23].

The ligands around Mn(2) are: three (μ_3-O) and three (bridging COO^-). The six ligands around Mn(3) are: three (μ_3-O), one (μ_2-O) and two bridging COO^-. As a hard group, four μ-O could stabilize manganese (IV) [22,23]. The ligands around Mn(4) are: one (μ_4-O), one (μ_2-O), two (bridging COO^-) and two water molecules (H_2O). These two water molecules are very important and one of them may serve as one of the substrates for water oxidation. In the recent structure of the WOC, Ca has seven ligands, three μ_3-O, two bridging COO^- and two H_2O molecules [22,23]. Similar to H_2O molecules coordinated to Mn(4), these two H_2O molecules are very important, and one of them may serve as the substrate for water oxidation [22,23]. The location of the substrate water binding sites on the $CaMn_4O_5(H_2O)_4$ inorganic core has been an important question in the study of the mechanism of water oxidation.

Many manganese compounds have been synthesized with the aim of simulating the WOC of PSII not only because the WOC consists of four manganese ions but also because manganese is of low cost and is environmentally friendly [22,23]. Few manganese complexes have been discovered so far that are able to catalyse water oxidation. However, manganese oxides as heterogeneous catalysts show promising activity towards water oxidation in the presence of non-oxo transfer oxidants.
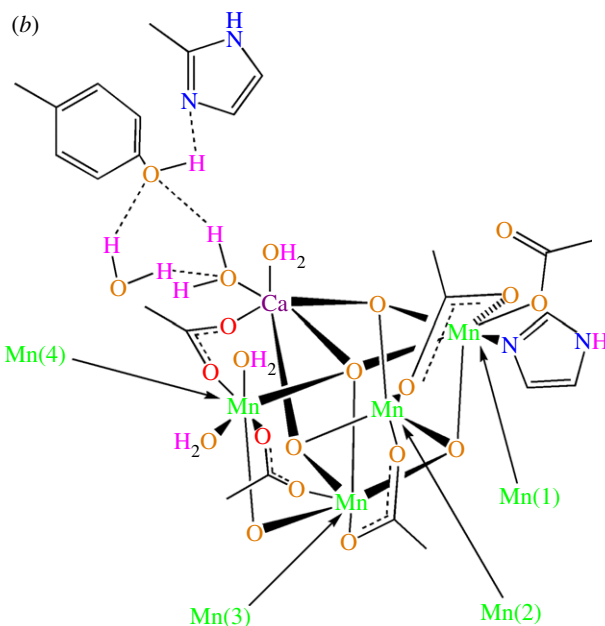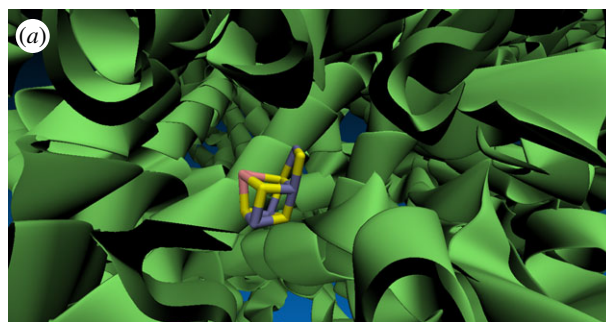

Figure 1. The whole structure of the $CaMn_4O_5(H_2O)_4$ cluster resembles a distorted chair, with the asymmetric cubane. There is only a small fraction of the residues that come in direct contact with the manganese–calcium cluster. In other words, the structure could be considered as a nano-sized manganese–calcium oxide in protein environments. The image was made with visual molecular dynamics (VMD) and is owned by the Theoretical and Computational Biophysics Group, NIH Resource for Macromolecular Modelling and Bioinformatics, at the Beckman Institute, University of Illinois at Urbana-Champaign. (*a*) The original data for figure 1 are from Kamiya & Shen [18] (PDB: 3ARC). (*b*) $CaMn_4O_5(H_2O)_4$ cluster and the surrounding amino acids. (Online version in colour.)

One of the most important oxidants in water oxidation experiments is tris(2,2′-bipyridyl) ruthenium (III) ($[Ru(bpy)_3]^{3+}$) [24]. A photoinduced oxidation of manganese oxides in the presence of the photosensitizer, $[Ru(bpy)_3]^{2+}$, in an aqueous solution needs the use of a sacrificial oxidant that is irreversibly reduced, allowing the net conversion of $[Ru(bpy)_3]^{2+}$ into $[Ru(bpy)_3]^{3+}$. $[Ru(bpy)_3]^{3+}$ can then act as an oxidant towards compounds by an intermolecular electron transfer because the potential of the $[Ru(bpy)_3]^{2+}/[Ru(bpy)_3]^{3+}$ redox couple in an aqueous solution is $E_{1/2} = 1.23$ V versus NHE. In other words, the excited sensitizer, $[Ru(bpy)_3]^{2+}$, is oxidized to $[Ru(bpy)_3]^{3+}$, which pulls an electron from the multi-electron manganese oxide catalyst, and then on the surface of the catalyst, two water molecules are oxidized to form one oxygen molecule [24]. Peroxodisulphate, $S_2O_8^{2-}$, or $[Co(NH_3)_5Cl]^{2+}$

(a)

(b)
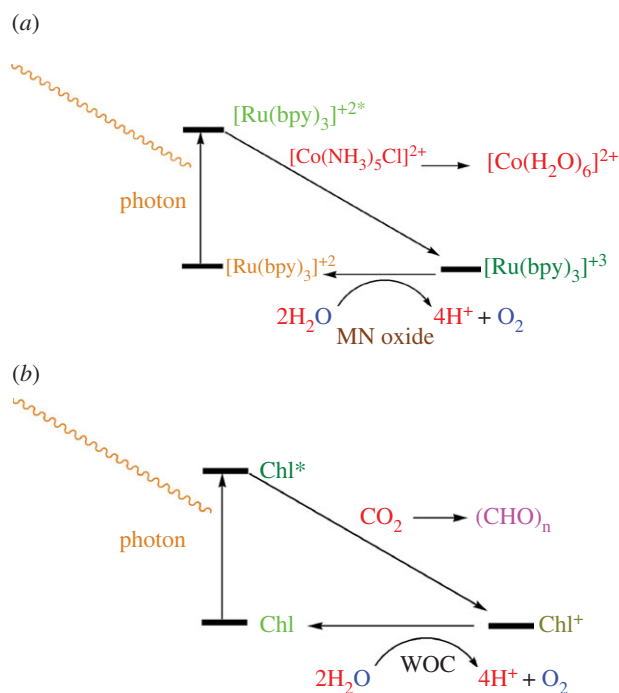
Scheme 2. A comparison of the reactions involved in water oxidation in the presence of (*a*) $[Ru(II)(bpy)_3]^{3+}$ and (*b*) chlorophyll. The biological water oxidation process involves three basic steps. First, trapping of light energy by chlorophyll pigments and rapid energy transfer to the reaction centre Chl, resulting in its oxidation to Chl^+. Second, rapid electron donation to Chl^+, through an oxidizable protein side-chain tyrosine 161 in D1 peptide. Third, oxidation of water to molecular oxygen within the WOC. (Online version in colour.)

are two irreversible electron acceptors used commonly in the literature to photogenerate $[Ru(bpy)_3]^{3+}$ in an aqueous medium (scheme 2*a*). A comparison of the reactions involved in oxygen evolution from water in the presence of $[Ru(II)(bpy)_3]^{2+}/[Co(NH_3)_5Cl]^{2+}$ and natural water oxidation is shown in scheme 2*b*. The resulting oxygen evolution molecules are quantitatively analysed by an oxygen meter or by a GC-MS equipment.

Another usual oxidant in water oxidation is cerium (IV) ammonium nitrate (Ce(IV)). Ce(IV) is a non-oxo transfer and strong one-electron oxidant. It is widely used as the primary oxidant in the oxidation of water to dioxygen catalysed by ruthenium and manganese compounds because of its solubility and stability in water in the absence of catalysts [24–29]. Previous results by membrane-inlet mass spectrometry (MIMS) have shown the production of isotopologues of molecular oxygen in reactions of manganese oxides with H_2O_2, HSO_5^-, Ce(IV) and $[Ru(bpy)_3]^{3+}$ in ^{18}O-enriched aqueous solutions [30]. These results show that oxygen evolution of reactions of Ce(IV) or $[Ru(bpy)_3]^{3+}$ is a 'real water oxidation' [30]. In other words, the results showed that in the case of H_2O_2, the bulk water is not involved in the O=O bond formation. Oxygen evolution in the presence of HSO_5^- is an oxygen-transfer reaction, and the water molecules participate in the O=O bond formation either through nucleophilic attack or through oxido-exchange pathways [30].

Many manganese complexes [31–38] were reported as models for the WOC in PSII but according to $H_2^{18}O$ isotope-labelling experiments coupled with membrane inlet mass spectrometry, only few manganese complexes discovered so far are able to act as catalysts for oxygen evolution.

Some other metal-based catalysts have been reported as promising catalysts for water oxidation but most of the synthetic compounds active in water oxidation are based on expensive metals and often on potentially carcinogenic salts [39].

The $CaMn_4O_5(H_2O)_4$ cluster in PSII could be considered as a nano-sized cluster of manganese oxide in a protein environment [40]. Thus, nano-sized manganese oxides are reported as good structural and functional models for the cluster. The nanometre-size of these particles ensures that most of the active sites are at the surface, where they function as a water-oxidizing catalyst [40–57].

A nano-sized compound could be defined as a particle with size in range of 1–100 nm (10^2–10^7 atoms) from zero to three dimensions. A nano-sized compound could exhibit unique physiochemical properties when compared with the bulk compound. As discussed by Maier [58], two types of size effects may be distinguished at nanoscale when compared with bulk compounds: first the effects that rely on increased surface-to-volume ratio; second, the true-size effects, which also involve changes of local materials properties.

Nanoscale particles could have completely different redox potential when compared with bulk material. Navrotsky's group reported that nanophase transition metal oxides show large thermodynamically driven shifts in oxidation–reduction equilibria [57]. This effect could change redox potential of nano-sized manganese as well as the water-oxidizing activity of nano-sized manganese oxide when compared with bulk manganese oxides [57].

2. NANO-SIZED MANGANESE OXIDES AS BIOMIMETIC CATALYSTS FOR WATER OXIDATION

2.1. Colloidal manganese oxide

In 1987, Harriman's group reported colloidal manganese oxide prepared by gamma radiolysis of aqueous solutions of $Mn(ClO_4)_2$ saturated with N_2O [29].

The absorption spectrum of the colloidal MnO_2 showed a clear peak at 330 nm. Light-scattering experiments suggested an initial particle diameter of 6 ± 1 nm, and kinetic considerations showed a diameter of 4.2 nm [29]. Aggregation occurred upon prolonged standing, and after 3 months, a polydispersed material with average particle diameter of approximately 70 nm was obtained. The colloidal MnO_2 had a negative surface charge, as demonstrated by electrophoresis, at pH > 3 and no change in absorption spectra was noted within the pH range of 3–12. Oxygen evolution experiments were made with freshly prepared materials [29]. However, the compound is a poor oxygen-evolving catalyst because it gives a very low total yield

(representing only 17.6% of the total number of oxidizing equivalents) and a slow rate of oxygen evolution.

2.2. Nanostructured manganese oxide clusters supported on mesoporous silica

Frei's group reported that nanostructured manganese oxide clusters supported on mesoporous silica efficiently evolved oxygen in an aqueous solution under mild conditions [49]. Manganese oxide clusters are exclusively formed inside the silica host and do not disrupt the cubic mesopore structure. The approximated spherical clusters had mean diameters in the $73–86$ nm range, depending on the calcination temperature, with narrow size distributions. Manganese K-edge X-ray absorption spectroscopy showed that materials calcined at $500°C$ feature mainly Mn(IV), while the mean Mn oxidation state decreases gradually towards higher calcination temperature, from Mn(III) at $600°C$ (corresponding to Mn_2O_3) to Mn(II,III) for the sample calcined at $900°C$. In other words, the experiments indicated that the contribution of MnO_2 reaches a maximum at $500°C$, while that of the spinel phase (Mn_3O_4) contributes significantly only above $600°C$ and then increasingly so towards higher temperatures. The Mn_2O_3 phase, on the other hand, is dominant between $600°C$ and $700°C$, and then declines. XANES spectra of micrometre-sized β-MnO_2, α-Mn_2O_3 and Mn_3O_4 particles were used for Mn K-edge fitting [49]. Thus, an increase in the calcination temperature reduces Mn(IV) to Mn(III), and a temperature above $700°C$ reduces Mn(IV) partially to Mn(II). The group showed that the mixed phase Mn oxide nanoclusters inside silica scaffolds are efficient catalysts for oxygen evolution from water, operating under mild pH conditions at room temperature and at a modest over-potential of 350 mV ($E°([Ru(bpy)_3]^{+3}/ ([Ru(bpy)_3]^{+2} = 1.23$ V, $E°(O_2/H_2O) = 0.89$ V at pH 5.6) [49]. The material calcined at $600°C$ is the most efficient catalyst towards water oxidation. The main phase in the compound is Mn_2O_3. The turnover frequency (TOF; the number of moles of substrate that a mole of catalyst can convert per unit time) they obtained is equal to 1630 s^{-1} per Mn oxide nanocluster for Mn oxide on mesoporous silica calcined at $400°C$, 1210 s^{-1} ($500°C$), 3330 s^{-1} ($600°C$), 1260 s^{-1} ($700°C$), 1590 s^{-1} ($800°C$) and 1830 s^{-1} ($900°C$). Compared with bulk material, the oxygen yield obtained by an aqueous suspension of micrometre-sized Mn_2O_3 is 26 times smaller. The group concluded that nanometre-sized manganese oxide clusters supported on a mesoporous silica scaffold have been established as efficient water oxidation catalysts in an aqueous solution at room temperature and at a pH of 5.8 [49]. The high surface area silica support may be critical for the integrity of the catalytic system because it offers a perfect, stable dispersion of the nanostructured manganese oxide clusters [49]. In addition, they suggest that the silica environment may play an important role in sustaining activity by protecting the active manganese centres of the catalyst from deactivation through surface restructuring and also that silica support may assist in deprotonation during photocatalysis, which avoids a

highly acidic environment surrounding the manganese catalytic site and stabilizes the manganese catalyst against leaching [49].

2.3. Soluble form of nano-sized colloidal manganese (IV) oxide

In 1989, Perez-Benito *et al.* [59] reported a soluble form of colloidal manganese (IV) by a simple method equation (2.1):

$$8MnO_4^-(aq) + 3S_2O_3^{2-}(aq) + 2H^+(aq)$$
$$\rightarrow 8MnO_2(s) + 6SO_4^{2-}(aq) + H_2O(1). \qquad (2.1)$$
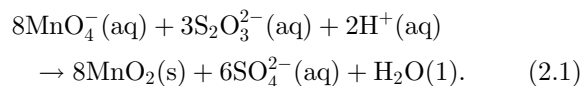
The colloidal particles are roughly spherical shaped with a radius of around 50 nm of manganese (IV) with negative electrostatic charge that stabilizes them in solution [59] (figure 2). The compound was used for oxidizing some organic compounds [60,61]. Recently, the colloidal manganese (IV) was used as a catalyst for oxygen evolution in the presence of oxone, H_2O_2, cerium (IV) ammonium nitrate (Ce(IV)) and $[Ru(bpy)_3]^{3+}$ [62]. The compound showed efficient water oxidation activity in the presence of $[Ru(bpy)_3]^{3+}$ or Ce(IV). The group found that the water-oxidizing activity of the compound is much more than bulk MnO_2 or α-Mn_2O_3 in the reported condition. The small size, dispersivity and charge of particles in this colloidal MnO_2 could be important factors in high rates of oxygen evolution by the compound in the presence of different oxidants [62].

2.4. Nano-size-layered manganese–calcium oxides

Recently, with the aim of simulating the $CaMn_4O_5(H_2O)_4$ cluster in PSII, it has been shown that the incorporation of calcium ions to manganese oxides can improve the catalytic activity of synthetic manganese oxides [45]. These readily synthesized layers of manganese–calcium oxides are efficient catalysts of water oxidation and are the closest structural and functional analogues to the native PSII catalyst found so far [46]. However, the molecular modelling of the $CaMn_4O_5(H_2O)_4$ cluster in PSII shows that it has a dimension of about approximately 0.5 nm [40]. Thus, nano-scale, and more interesting ångström-scale, manganese or manganese–calcium oxides will be better structural and functional models for the $CaMn_4O_5(H_2O)_4$ in PSII. Nano-sized amorphous manganese–calcium oxide has been synthesized and its water oxidation activity in the presence of cerium (IV) ammonium nitrate was reported. The nano-sized amorphous manganese–calcium oxide is very closely related to the water-oxidizing cluster in PSII, not only because of similarity in the elemental composition, oxidation number of manganese ions, similarity of structure and function to $CaMn_4O_5(H_2O)_4$ cluster in PSII, but also because of more similar catalyst particle size when compared with previously reported micro-size amorphous manganese–calcium oxides [40]. The oxide was amorphous, and XRD data for the compound were of very poor resolution. However, the peak near the 2.4 Å spacing ($\theta \sim 19$)—observed in all octahedrally
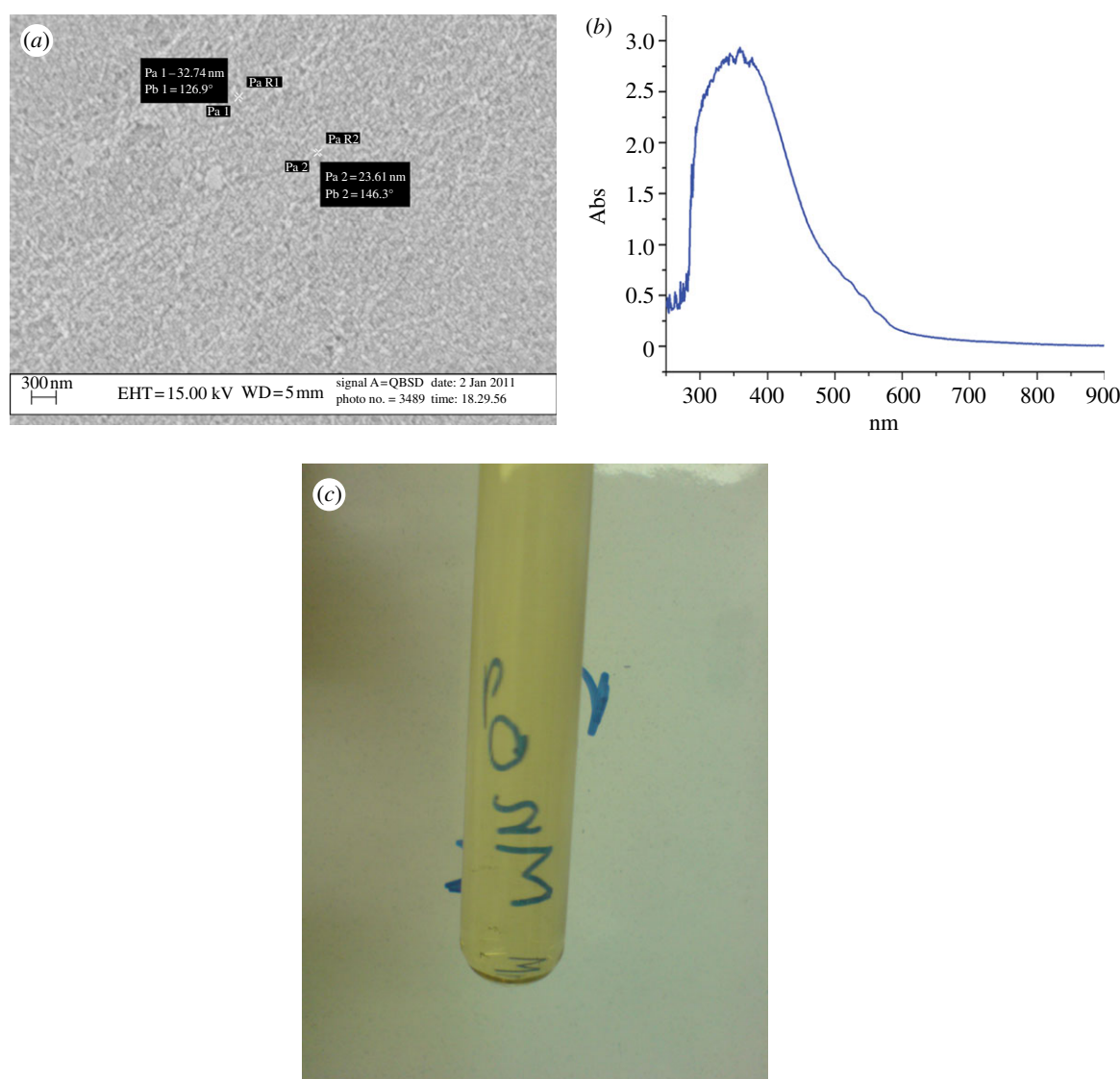
Figure 2. (*a*) SEM micrographs of particles after the aggregation of colloidal particles. (*b*) Visible spectrum of soluble form of nano-sized colloidal manganese(IV) oxide. An image of soluble form of nano-sized colloidal manganese(IV) oxide in a tube. (Online version in colour.)

coordinated manganese oxide materials—and the peak near 7.0 Å ($\theta \sim 5.5$)—found in most layered materials such as birnessite—were observed in XRD patterns of this compound, and are related to corresponding values of the previously reported structure of similar compounds [40]. Scanning electron microscopy (SEM) showed that the compound consists of particles of at least less than 50 nm in size. The layered structure of these compounds could be the transmission electron microscopic (TEM) analysis images (figure 3).

The TOF (mol O_2 per mol Mn per second) of the compound in the presence of a 0.45 M solution of Ce(IV) was approximately 0.002, that is approximately four times more than the best TOF (mol O_2 per mol Mn per second) reported for the manganese compound [40]. The oxide could be used for several times (at least for five times) without any significant loss in its reactivity. The nano-size amorphous manganese–calcium oxide is one of the best manganese compounds towards water oxidation. Calcium and manganese are of low cost and are environmentally friendly; these compounds

could be a good candidate for water-oxidizing catalyst in artificial photosynthesis [40]. Recent results showed that cations between manganese oxide-layers in layered manganese oxides are not an important factor in water-oxidizing activity of these oxides; however, water content, crystallinity, size and surfaces of particles, dispersion of particles in solution, and temperature the samples are calcined are more important factors in water-oxidizing activity of manganese oxides [63]. Comparing with other manganese oxides, the efficiency of layered manganese oxides could be related to the open structure and small particle size of these oxides because of the incorporation of calcium, aluminium, zinc or other cations in the structure. A mechanism proposed by the group is shown in scheme 3 [63].

2.5 Water oxidation by nano-sized λ-MnO₂

Dismukes's group reported the water-oxidizing activity of nano-sized λ-MnO₂ [51]. The compound was prepared by the reaction of Mn(OAc)₂ with LiNO₃ at

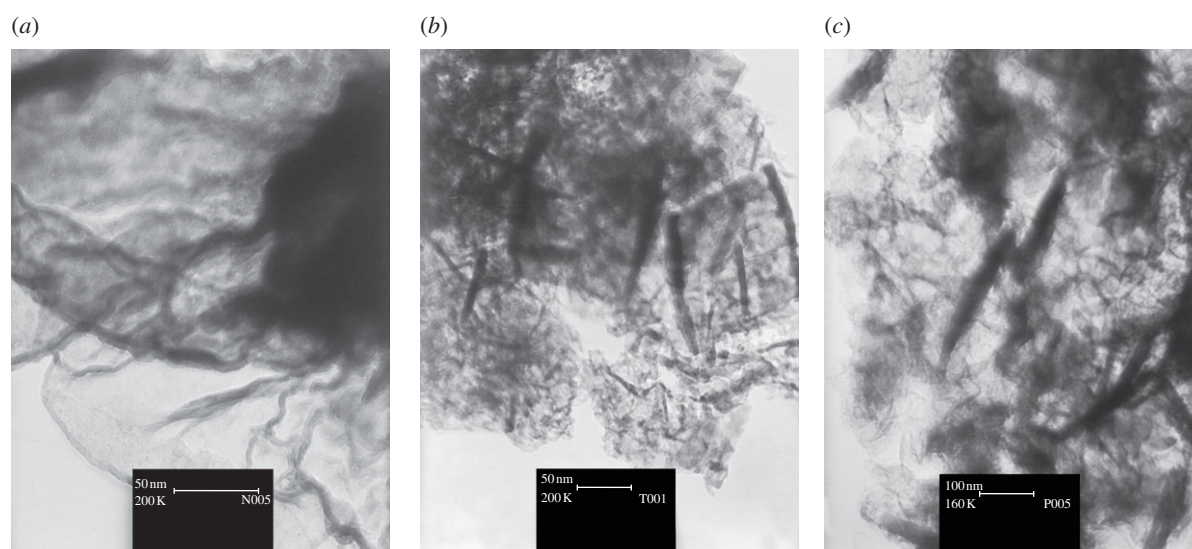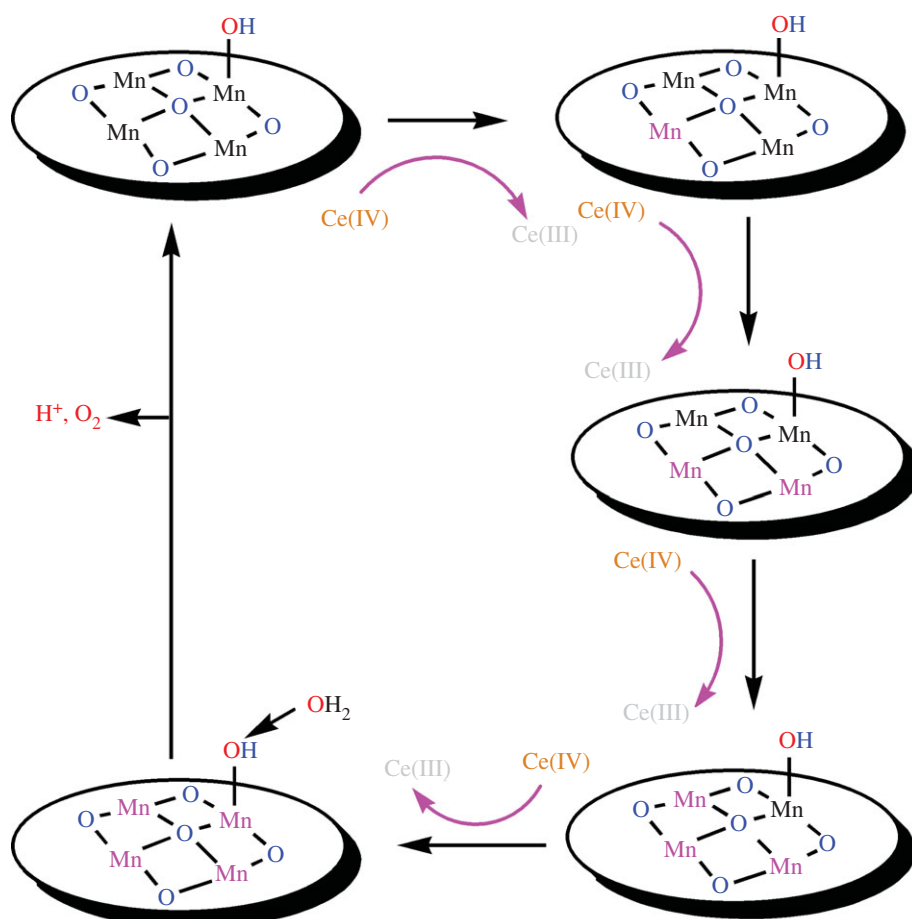(a)   (b)   (c)

Figure 3. TEM images of (*a*) nano-sized layered aluminium−manganese, (*b*) layered manganese−calcium and (*c*) layered zinc−manganese oxides.

Scheme 3. The proposed mechanism of water oxidation in the reaction of manganese oxides and Ce(IV) or $[Ru(bpy)_3]^{3+}$ as an oxidant. Proposed role(s) of calcium, aluminium or zinc could be facilitating high oxidation states and/or the formation a moderate structure for water oxidation at manganese oxides. Oxidized manganese ions are shown in pink. (Online version in colour.)

350°C in the presence of urea and citrate in acidic solution to aid in forming a higher surface area material during degassing of H_2O, NH_3 and CO_2 [51]. Delithiation of nanocrystalline spinel $LiMn_2O_4$ by dilute HNO_3 solution treatment produced nano-sized λ-MnO_2 (20−100 nm). $LiMn_2O_4$ is not a catalyst for water oxidation, but upon removal of the lithium, the cubical Mn_4O_4 cores become active sites for oxidizing water to molecular oxygen, which was investigated with the photochemical $Ru(bpy)_3]^{+3}/S_2O_8^{2-}$ system at

pH = 5.8. Dismukes's group introduced the cubical Mn_4O_4 units in λ-MnO_2 indirectly, similar to the manganese–calcium cluster of the WOC of PSII [51].

2.6. Nano-structured MnO₂

MnO_2 is known as an oxidant and has good stability in acidic conditions [64]. Among different major polymorphs of MnO_2, α-MnO_2 has the largest channels, formed by 2 × 2 edge-shared Mn octahedra and, therefore, it shows significant advantages for the uptake of guest cations compared with other MnO_2 polymorphs. Recently, Jiao's group reported α-MnO_2 nanotubes, α-MnO_2 nanowires and β-MnO_2 nanowires as catalysts for water oxidation driven by visible light [56,64]. The SEM image clearly shows that the morphology of the as-prepared α-MnO_2 nanotubes is highly uniform, with a tube outer diameter of approximately 100 ± 30 nm and an inner diameter of approximately 40 ± 20 nm [64]. The length of the nanotubes was approximately 0.5–3 mm. SEM images of the β-MnO_2 nanowires confirmed that the nanowire morphology, with a typical length of 2 ± 1 mm and a diameter of 30 ± 20 nm, occurs throughout this sample. The short rod α-MnO_2 particles with a length of 200 ± 50 nm and a width of 70 ± 30 nm were observed by SEM analysis. The results by the energy-dispersive X-ray spectroscopy (EDX) measurements showed that the as-synthesized nanotubes contain about approximately 10.5 atomic % potassium cations in both the α-MnO_2 nanotubes and nanowires, while no potassium was observed in the bulk α-MnO_2 and β-MnO_2 nanowires [64]. The highly crystalline nature of the α-MnO_2 nanotubes, α-MnO_2 nanowires and β-MnO_2 nanowires was observed by the high-resolution transmission electron microscopy (HRTEM) images [64]. They performed water oxidation experiments using $[Ru(bpy)_3]^{2+}$/$S_2O_8^{2-}$ system [64].

The crystal structure of these catalysts has a negligible effect on its water oxidation reactions by comparing nanostructured α-MnO_2 and β-MnO_2 with other polymorphs of MnO_2 that have been recently reported as water oxidation catalysts [64]. A TOF of 0.035 (mol O_2 per mol Mn per second) was observed for the α-MnO_2 nanotubes, and the TOF for α-MnO_2 nanowires, bulk α-MnO_2 and β-MnO_2 nanowires were 0.059, 0.01 and 0.02, respectively. To find more about the origin of the difference between the water oxidation activities of these compounds, the authors measured their surface area by a nitrogen adsorption analysis (Brunauer–Emmett–Teller, BET). On the basis of these results, it is observed that the TOF per surface of these manganese oxides is similar even with the different morphologies (nanotubes or nanowires) and crystal structures (α-MnO_2 or β-MnO_2). In other words, the Mn ions on the surface of catalyst in all three oxides exhibit similar water oxidation activity. Authors also compared their results with the Mn oxides previously reported as water oxidation, and found that irrespective of morphologies and crystalline structures of MnO_2 catalysts, most of the manganese dioxides exhibit a similar TOF per surface. They concluded that the morphology and crystal structure have

negligible effects on the water oxidation activity of the MnO_2 catalysts, but the surface area is an important factor in water oxidation activity.

2.7. A very simple method to synthesize nano-sized manganese (III) oxide

Nano-sized manganese oxides are known to be useful, versatile and environmentally friendly catalysts for important reactions, and there are many methods for the synthesis of these compounds [65–68]. Among them, solvothermal, polymeric-precursor and surfactant-mediated routes are quite popular. Decomposition of manganese nitrate depends on some factors such as heating rate, moisture content of the atmosphere or manganese nitrate, and different decomposition temperatures, mechanisms and intermediates are reported for the reaction. In air (or in the presence of oxygen) manganese nitrate decomposes up to 200–220°C. In moist atmosphere, the decomposition of the nitrates can occur at lower temperatures and more interestingly, hydrated manganese nitrate has been reported to decompose at lower temperatures than dehydrated one. Recently, Najafpour's group prepared nano-sized particles of Mn_2O_3 by a very simple and low-cost process, using a decomposing aqueous solution of manganese nitrate at 100°C. The X-ray diffraction (XRD) pattern of as-prepared manganese oxide showed that the compound is α-Mn_2O_3. SEM images determined that the compound consists of particles of less than 100 nm in size (figure 4) [65]. Transmission electron microscopy (TEM) images allowed us to determine that the compound consists of both amorphous and crystalline phase. The compound acts as an efficient catalyst for water oxidation (0.15 mmol O_2/mol Mn.s) in the presence of Ce(IV). A plot of ln k_o (water oxidation) versus T^{-1} was linear and gave E_a = 96 KJ as apparent activation parameters for water oxidation reaction of the nano-sized manganese oxide. The oxygen evolution rate increases with increasing concentration of Ce(IV). The increase in the oxygen evolution rate in low concentration of Ce(IV) is fast in the Ce(IV) concentration range of 0.01–0.1 M. However, in higher concentrations of Ce(IV), the slope of the increasing the oxygen evolution rate is slow (is less steep) [65].

The nano-sized manganese (III) oxide also showed a high activity in epoxidation of aromatic olefins and a mild activity in the epoxidation of some non-aromatic olefins in the presence of H_2O_2 and bicarbonate ion [65].

2.8. Nano-sized manganese oxide–bovine serum albumin

Manganese oxides have been reported as a heterogeneous catalyst for water oxidation by a few groups. However, unlike PSII, these synthetic structural and functional models contain no amino acid groups to stabilize manganese oxide, proton transfer or/and decrease the activation energy for water oxidation. In PSII, there are specific intrinsic proteins that appear to be required for water oxidation. These are proteins CP47, CP43, the D1 protein, the D2 protein and the
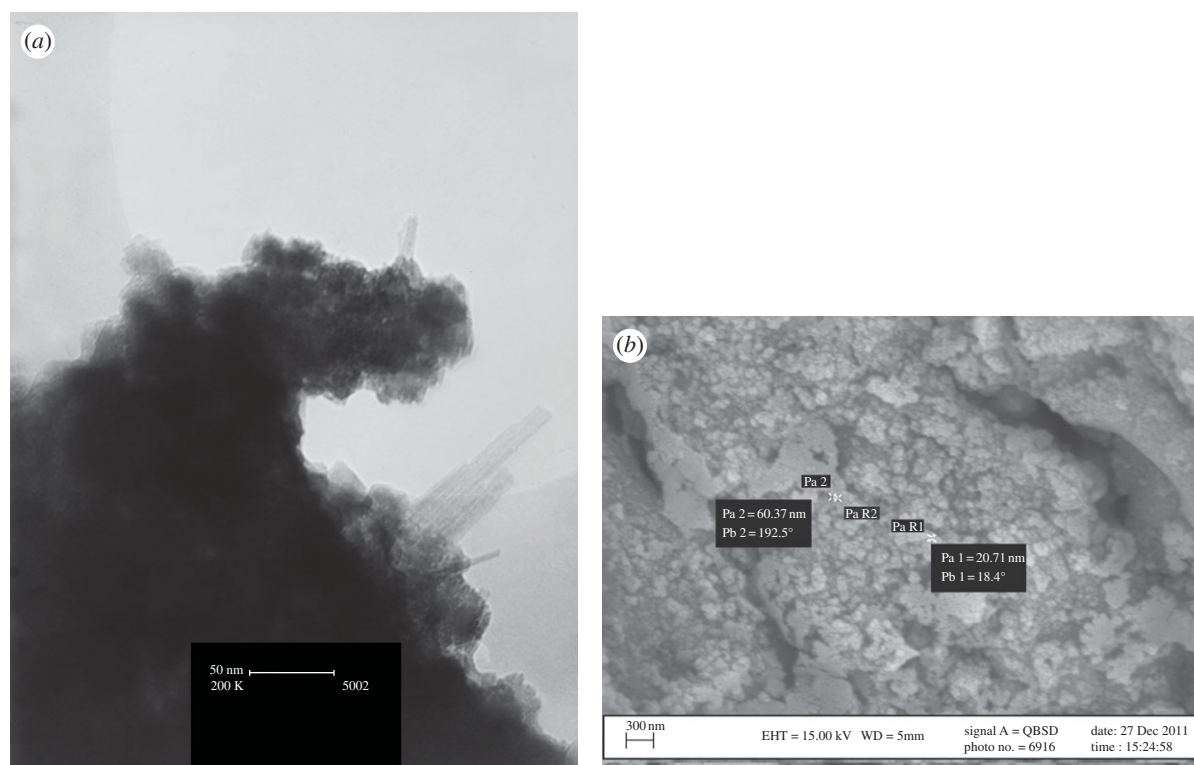
Figure 4. (*a*) SEM and (*b*) TEM images of manganese oxide prepared by decomposition of manganese nitrate solution at 100°C for 24 h.

α and β subunits of cytochrome b_{559} [11–19,69–74]. Thus, PSII consists of hundreds of amino acids. However, there is only a small fraction of the residues that come in direct contact with the manganese–calcium cluster. Many amino acids in PSII are involved in proton, water or oxygen transfer. Roles for the residues that come in direct contact with the manganese–calcium cluster could include regulation of charges and electrochemistry of the manganese cluster, and help in coordinating water molecules at appropriate metal sites or/and in maintaining the stability of this cluster [69–74]. Manganese stabilizing protein in PSII is a conserved extrinsic component of the WOC, and its deletion from the photosystem could cause a dramatic lowering of the rate of water oxidation [69–74]. In addition to stabilizing the Mn-Ca cluster or/and decreasing the activation energy for water oxidation, it could be important in linking the active site of the WOC with the lumen and be involved in a proton transfer network. Recently, Najafpour *et al.* reported a nano-sized manganese oxide–bovine serum albumin (BSA) as a simple structural and functional model for the WOC in PSII [75]. BSA is one of the most studied proteins that has a strong affinity for a variety of inorganic molecules binding to different sites. BSA is a soluble protein in plasma of the circulatory system and acts in transport and deposition of endogenous and exogenous substances. Albumin can readily undergo conformational changes, and it is classed as a soft protein owing to its relatively flexible structure. A three-dimensional image of serum albumin molecule is shown in figure 5.

BSA has been used as a simple model for stabilizing protein in PSII. The nano manganese oxide–BSA was synthesized by a very simple method [75] involving the reaction of a solution of manganese (II) chloride with a solution of BSA in water. Then KMnO₄ was added to the solution under stirring. Drying the solution in air and at room temperature produced a homogeneous nano-sized manganese oxide–BSA film. The charge, van der Waals forces, Columbic forces, hydrophobic interactions, the sorbate conformational stability and the surface area that the particle provides are important factors for the interaction of a protein and a compound. Nano manganese oxide–BSA both in solution and as a film show water-oxidizing activity [75]. The brown solution was characterized by UV-Vis, SEM, TEM, IR, AFM and XRD. As demonstrated by the TEM images, very small particles of nano-sized manganese oxide are attached to the BSA protein [75]. In the compound, manganese oxide is amorphous, and a specific phase could not be identified by XRD [75]. AFM images show that nucleation (white area) occurs on special locations most probably near imidazole and carboxylate groups [75].

The water oxidation activity of the compound was studied. The results show that BSA not only induces the nucleation, but also inhibits the further growth of manganese oxide as larger particles are formed without BSA [75]. Moreover, dispersion of manganese oxide in water is unique and may also increase the rate of reaction of particles with reactants, and could result in a high rate of many reactions [75].

In the nano-sized manganese oxide–BSA compound, manganese oxide is amorphous and a specific phase could not be identified by XRD. In this study, $[Ru(bpy)_3]^{+2}/K_2S_2O_8$ was used as an oxidant system for water oxidation. During irradiation with visible light ($\lambda > 400$ nm), oxygen evolution was observed upon
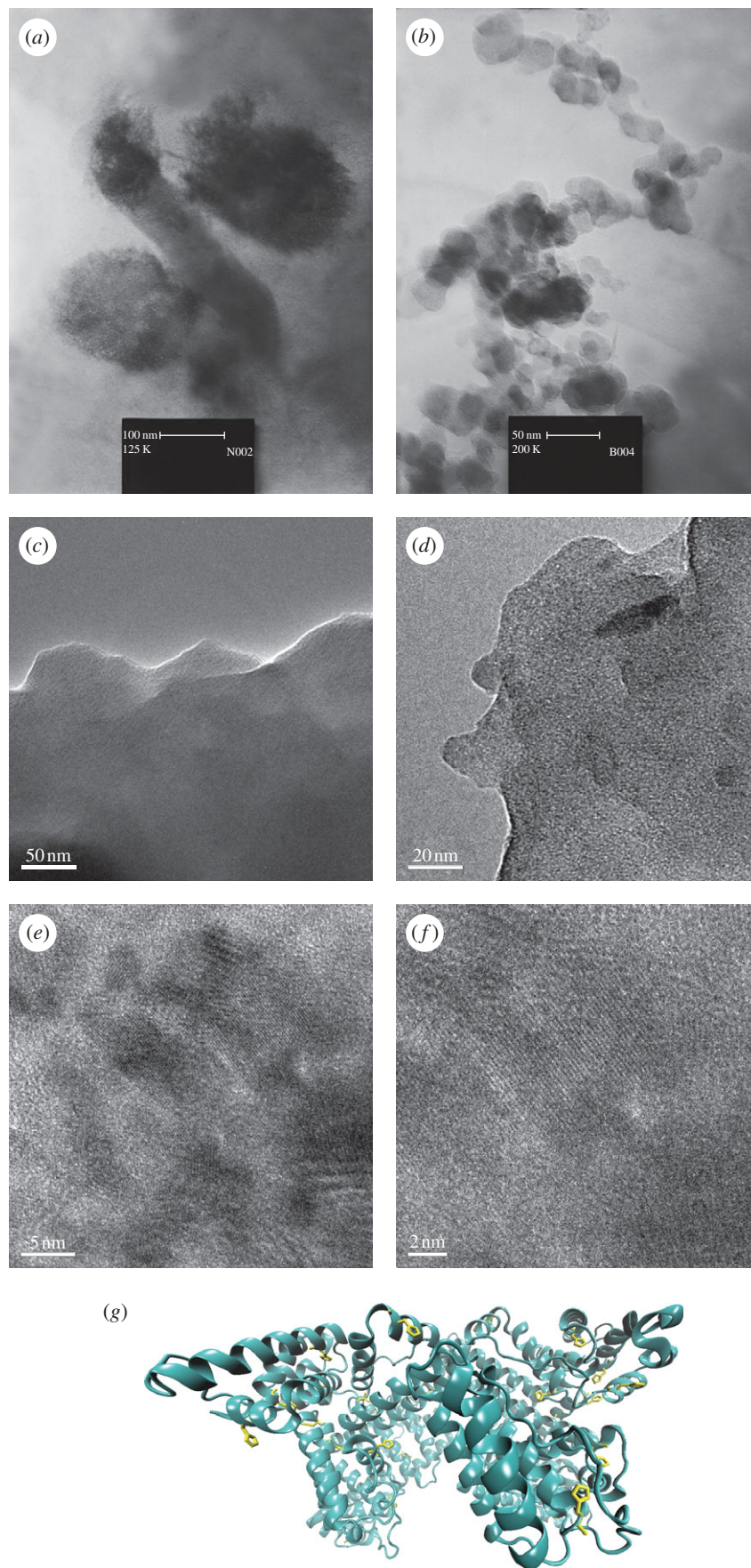
Figure 5. TEM images of the manganese oxide prepared in the presence of (*a,b*) BSA, (*c,d*) manganese oxide–BSA film and (*e,f*) HRTEM images of manganese oxide–BSA film. (*g*) A three-dimensional image of bovine serum albumin molecule. Imidazole groups as proposal sites for interaction with manganese ions are shown in yellow. (Online version in colour.)

adding the nano manganese oxide—BSA compound to an aqueous solution containing $[Ru(bpy)_3]^{2+}$ and $K_2S_2O_8$. Intensity of light was less than one-tenth of a bright sunny day (on a bright sunny day the illumination can be more than 100 000 lux) [75]. The oxygen evolution rate of this compound in this condition is 140 μmol_{O2} $mol_{Mn}^{-1}\,s^{-1}$. The nano-sized manganese oxide–BSA is also a good catalyst for water oxidation in the presence of Ce(IV) (figure 5) [75]. The oxygen evolution rate of this compound in the presence of Ce(IV) (0.1 M) is 270 $\mu mol_{O2}\,mol_{Mn}^{-1}\,s^{-1}$. Compared with water oxidation activity of other manganese oxides, the nano manganese oxide–BSA materials are good catalysts for water oxidation, thus showing that incorporation of manganese oxides into BSA can improve the water oxidation activity of these compounds [75]. At least, BSA could help in the dispersion of these nanoparticles in solution, and the dispersivity of particles in water could increase the rate of reaction of particles with oxidants (Ce(IV) or $[Ru(bpy)_3]^{+3}$). In a real artificial photosynthetic system, water oxidation catalysis has to be coupled to other electron acceptor materials than Ce(IV) or $[Ru(bpy)_3]^{3+}$ because Ce(IV), or even $[Ru(bpy)_3]^{3+}$, is a very powerful oxidant ($E° > +1.4$ V versus the standard hydrogen electrode (SHE)) and could oxidize and decompose amino acids of BSA, or other ligands in related compounds [76–78]. In biological water oxidation, the WOC is linked to the reaction centre II chlorophyll via a redox-active tyrosine residue on the D1 subunit, labelled as Y_Z. The residue oxidizes the WOC, and the $Yz^{+\cdot}/Yz$ potential is only approximately 1.0 V versus SHE (for more details, see [13,14]).

2.9. Amorphous manganese oxide

Mixed valent porous amorphous manganese oxide is an active catalyst for oxidation of many organic compounds. The compound could be prepared at room temperature by the reduction of $KMnO_4$ with oxalic acid. Specifically, 1.58 g of $KMnO_4$ was dissolved in 60 ml distilled deionized water (DDW) and 2.28 g of oxalic acid was dissolved in 100 ml DDW [79]. The potassium permanganate solution was then added dropwise to the oxalic acid solution. The resulting reaction mixture was continuously stirred for 2 h at room temperature [79]. The brown slurry was filtered, and the product obtained was washed several times with deionized water and dried overnight at 90°C. The procedure is simple and produced an efficient catalyst (0.54 mmol O_2/mol Mn.s and total turnover number of 290 mmol O_2/mol Mn after 1 h) for water oxidation in the presence of Ce(IV) and $[Ru(bpy)_3]^{+2}/K_2S_2O_8$ as oxidants, as reported by Suib and Dutta groups [79]. $H_2^{18}O$ labelling studies proved that water was the source of dioxygen [79].

The reusability of the catalyst was also tested. The catalyst was washed several times to remove any cerium ions. The regenerated catalyst was reusable without loss of catalytic activity and gave equivalent turnover numbers as the fresh catalyst [79]. A comparison of IR and XRD spectra of fresh and regenerated catalyst revealed that no observable phase change occurred after reaction [79].

Table 1. The rate of water oxidation by the various manganese oxides as catalysts for water oxidation.

compound	oxidant	TOF (mmol O_2/mol Mn)	references
$CaMn_2O_4.H_2O$ (nano particles)	Ce(IV)	2.2	[36]
$CaMn_2O_4.H_2O$	Ce(IV)	0.54	[41]
amorphous manganese oxides	$Ru(bpy)_3^{3+}$	0.06	[75]
	Ce(IV)	0.52	
$CaMn_2O_4.4H_2O$	Ce(IV)	0.32	[41]
nano manganese oxide–BSA	$Ru(bpy)_3^{3+}$	0.14	[71]
	Ce(IV)	0.27	
nano-sized α-Mn_2O_3	Ce(IV)	0.15	[61]
octahedral molecular sieves	$Ru(bpy)_3^{3+}$	0.11	[75]
	Ce(IV)	0.05	
MnO_2 (colloid)	Ce(IV)	0.09	[57]
α-MnO_2 nanowires	$Ru(bpy)_3^{3+}$	0.059	[60]
$CaMn_3O_6$	Ce(IV)	0.046	[24]
$CaMn_4O_8$	Ce(IV)	0.035	[24]
α-MnO_2 nanotubes	$Ru(bpy)_3^{3+}$	0.035	[60]
Mn_2O_3	Ce(IV)	0.027	[41]
β-MnO_2 nanowires	$Ru(bpy)_3^{3+}$	0.02	[60]
$Ca_2Mn_3O_8$	Ce(IV)	0.016	[47]
$CaMnO_3$	Ce(IV)	0.012	[47]
bulk α-MnO_2	$Ru(bpy)_3^{3+}$	0.01	[60]

Morphological studies using TEM showed that the compound consists of aggregates of nanoparticles, and a high-resolution TEM (HRTEM) image could show nanocrystallites with highly random orientation and crystallite sizes of less than 10 nm [79]. The far-IR region exhibits two broad features at 519 and 437 cm^{-1} related to Mn–O bands. In this compound, the average oxidation state of manganese is 3.91. Suib and Dutta groups related the high catalytic activity of the compound to its structure, which is a layered manganese oxide analogous to hexagonal birnessite with cation vacancies in the MnO_2 sheet [79]. Cation vacancies in the catalyst are influential in catalytic activity owing to coordinatively unsaturated oxygens, which are excellent sites for proton binding. This μ-OH unit thus created at vacancy or edge sites can undergo deprotonation and help in proton-coupled electron transfer during water oxidation catalysis [46,79]. In addition, smaller particle sizes (less than 10 nm) and high surface area result in larger number of edge sites than is available for water molecules to bind. The surface of the compound could also present more sites for the coordination of water molecules to the catalyst [79]. Similar to manganese–calcium cluster in PSII, a few, crystallographically characterized manganese–calcium complexes have also been reported [80–82]. The models were not discussed here, but they could be very important for our further understanding of the chemistry of manganese–calcium complexes.

3. CONCLUSIONS

Advances in the field of chemistry are making it possible to understand more about biological water oxidation and design as well as to synthesize a super

catalyst for water oxidation to develop artificial photosynthetic systems for hydrogen generation by water splitting. Choosing the correct metal [78,79,83–87] ion and finding suitable strategies [77–79,83–86] for water oxidation are important steps towards the goal. Nano-sized manganese oxides are promising compounds for water oxidation because the compounds are stable, economical, efficient, environmentally friendly and easy to use, synthesize and manufacture the catalyst (table 1). Using advanced strategies [78,79, 83–91] to design and synthesize metal oxides, the simple compound could present a fascinating area for further study that will reveal intriguing new scientific understanding and technological potential.

REFERENCES

1 Wydrzynski, T. & Hillier, W. (eds) 2011 *Molecular solar fuels.* Cambridge, UK: Royal Society of Cambridge.

2 Najafpour, M. M. (ed.) 2012 *Artificial photosynthesis.* Rijeka, Croatia: Tech Publications.

3 Pace, R. J. 2005 An integrated artificial photosynthesis model. In *Artificial photosynthesis from basic biology to industrial application* (eds A. F. Collings & C. Critchley), ch. 2. Weinheim, Germany: Wiley-VCH.

4 Reece, S. Y., Hamel, J. A., Sung, K., Jarvil, T. D., Esswein, A. J., Pijpers, J. J. H. & Nocera, D. G. 2011 Wireless solar water splitting using silicon-based semiconductors and earth-abundant catalysts. *Science* **334**, 645–648. (doi:10.1126/science.1209816)

5 Lewis, N. S. 2007 Toward cost-effective solar energy use. *Science* **315**, 798–801. (doi:10.1126/science.1137014)

6 Allakhverdiev, S. I. *et al.* 2010 Photosynthetic hydrogen production. *J. Photochem. Photobiol. C* **11**, 87–99.

7 Allakhverdiev, S. I., Kreslavski, V. D., Thavasi, V., Zharmukhamedov, S. K., Klimov, V. V., Nagata, T., Nishihara, H. & Ramakrishna, S. 2009 Hydrogen photoproduction by use of photosynthetic organisms and biomimetic systems. *Photochem. Photobiol. Sci.* **8**, 148–156. (doi:10.1039/b814932a)

8 Allakhverdiev, S. I. 2012 Photosynthetic and biomimetic hydrogen production. *Int. J. Hydrog. Energy* **37**, 8744–8752. (doi:10.1016/j.ijhydene.2012.01.045)

9 Allakhverdiev, S. I., Casal, J. & Nagata, T. 2009 Photosynthesis from molecular perspectives: towards future energy production. *Photochem. Photobiol. Sci.* **8**, 137–138. (doi:10.1039/b823060a)

10 Bard, A. J. & Fox, M. A. 1995 Artificial photosynthesis: solar splitting of water to hydrogen and oxygen. *Acc. Chem. Res.* **28**, 141–145. (doi:10.1021/ar00051a007)

11 Hotchandania, S., Ozdemir, U., Nasr, C., Allakhverdiev, S. I., Karacan, N., Klimov, V. V., Kamat, P. V. & Carpentier, R. 1999 Redox characteristics of Schiff base manganese and cobalt complexes related to water-oxidizing complex. *Bioelectrochem. Bioenerg.* **48**, 53–59. (doi:10.1016/S0302-4598(98)00235-9)

12 Nagata, T., Zharmukhamedov, S. K., Khorobrykh, A. A., Klimov, V. V. & Allakhverdiev, S. I. 2008 Reconstitution of the water-oxidizing complex in manganese. *Photosynth. Res.* **98**, 277–284. (doi:10.1007/s11120-008-9319-9)

13 Allakhverdiev, S. I., Tomo, T., Shimada, Y., Kindo, H., Nagao, R., Klimov, V. V. & Mimuro, M. 2010 Redox potential of pheophytin a in photosystem II of two cyanobacteria having the different special pair chlorophylls. *Proc. Natl Acad. Sci. USA* **107**, 3924–3929. (doi:10.1073/pnas.0913460107)

14 Allakhverdiev, S. I., Tsuchiya, T., Watabe, K., Kojima, A., Los, D. A., Tomo, T., Klimov, V. V. & Mimuro, M. 2011 Redox potentials of primary electron acceptor quinone molecule $(QA)^-$ and conserved energetics of photosystem II in cyanobacteria with chlorophyll a and chlorophyll d. *Proc. Natl Acad. Sci. USA* **108**, 8054–8058. (doi:10.1073/pnas.1100173108)

15 Zouni, A., Witt, H. T., Kern, J., Fromme, P., Krauss, N., Saenger, W. & Orth, P. 2001 Crystal structure of photosystem II from *Synechococcus elongatus* at 3.8 Å resolution. *Nature* **409**, 739–743. (doi:10.1038/35055589)

16 Ferreira, K. N., Iverson, T. M., Maghlaoui, K., Barber, J. & Iwata, S. 2004 Architecture of the photosynthetic oxygen-evolving center. *Science* **303**, 183–188. (doi:10.1126/science.1093087)

17 Guskov, A., Kern, J., Gabdulkhakov, A., Broser, M., Zouni, A. & Saenger, W. 2009 Cyanobacterial photosystem II at 2.9 Å resolution and role of quinones, lipids, channels and chloride. *Nat. Struct. Mol. Biol.* **16**, 334–342. (doi:10.1038/nsmb.1559)

18 Kamiya, N. & Shen, J. R. 2003 Crystal structure of oxygen-evolving photosystem II from *Thermosynechococcus vulcanus* at 3.7-Å resolution. *Proc. Natl Acad. Sci. USA* **100**, 98–103. (doi:10.1073/pnas.0135651100)

19 McEvoy, J. P. & Brudvig, G. W. 2006 Water-splitting chemistry of photosystem II. *Chem. Rev.* **106**, 4455–4483. (doi:10.1021/cr0204294)

20 Najafpour, M. M. 2006 Current molecular mechanisms of photosynthetic oxygen evolution. *Plant Biosyst.* **140**, 163–170. (doi:10.1080/11263500600756397)

21 Najafpour, M. M. 2009 A possible evolutionary origin for the Mn_4 cluster in photosystem II: from manganese superoxide dismutase to oxygen evolving complex. *Orig. Life Evol. Biosph.* **39**, 151–163. (doi:10.1007/s11084-009-9159-4)

22 Umena, Y., Kawakami, K., Shen, J.-R. & Kamiya, N. 2011 Crystal structure of oxygen-evolving photosystem II at a resolution of 1.9 Å. *Nature* **473**, 55–60. (doi:10.1038/nature09913)

23 Kawakami, K., Umena, Y., Kamiya, N. & Shen, J.-R. 2011 Structure of the catalytic, inorganic core of oxygen-evolving photosystem II at 1.9 Å resolution. *J. Photochem. Photobiol. B* **104**, 9–18. (doi:10.1016/j.jphotobiol.2011.03.017)

24 Morris, N. D. & Mallouk, T. E. 2002 A high-throughput optical screening method for the optimization of colloidal water oxidation catalysts. *J. Am. Chem. Soc.* **124**, 11 114–11 121. (doi:10.1021/ja017895f)

25 Najafpour, M. M., Kozlevcar, B., McKee, V., Jaglicic, Z. & Jagodic, M. 2011 The first pentanuclear heterobimetallic coordination cation with Ce^{III}, Ce^{IV} and Mn^{II}. *Inorg. Chem. Commun.* **14**, 125–127. (doi:10.1016/j.inoche.2010.10.002)

26 Ikeda-Ohno, A., Tsushima, S., Hennig, C., Yaita, T. & Bernhard, G. 2012 Dinuclear complexes of tetravalent cerium in an aqueous perchloric acid solution. *Dalton Trans.* **41**, 7190–7192. (doi:10.1039/C2DT12406H)

27 Najafpour, M. M. 2011 Hollandite as a functional and structural model for the biological water oxidizing complex: manganese–calcium oxide minerals as a possible evolutionary origin for the CaMn₄ cluster of the biological water oxidizing complex. *J. Geomicrobiol.* **28**, 714–718. (doi:10.1080/01490451.2010.515188)

28 Najafpour, M. M. 2011 Mixed-valence manganese calcium oxides as efficient catalysts for water oxidation. *Dalton Trans.* **40**, 3793–3795. (doi:10.1039/c0dt01109f)

29 Harriman, A., Richoux, M., Christensen, P. A., Mosseri, S. & Neta, P. 1987 Redox reactions with colloidal metal oxides. Comparison of radiation-generated and chemically generated RuO₂·2H₂O. *J. Chem. Soc. Faraday Trans.* **83**, 3001–3014. (doi:10.1039/f19878303001)

30 Shevela, D., Koroidov, S., Najafpour, M. M., Messinger, J. & Kurz, P. 2011 Calcium manganese oxides as oxygen evolution catalysts: O₂ formation pathways indicated by ¹⁸O-labelling studies. *Chem. Eur. J.* **17**, 5415–5423. (doi:10.1002/chem.201002548)

31 Najafpour, M. M. & Allakhverdiev, S. I. 2012 Manganese compounds as water oxidizing catalysts for hydrogen production via water splitting: from manganese complexes to nano manganese oxides. *Int. J. Hydrog. Energy* **37**, 8753–8764. (doi:10.1016/j.ijhydene.2012.02.075)

32 Yagi, M. & Kaneko, M. 2001 Molecular catalysts for water oxidation. *Chem. Rev.* **101**, 21–36. (doi:10.1021/cr980108l)

33 Kurz, P., Anderlund, M. F., Shaikh, N., Styring, S. & Huang, P. 2008 Redox reactions of a dinuclear manganese complex—the influence of water. *Eur. J. Inorg. Chem.* **5**, 762–770. (doi:10.1002/ejic.200700888)

34 Najafpour, M. M. & McKee, V. 2010 A dinuclear manganese (II) complex with 2,6-pyridinedicarboxylate: preparation, crystal structure and oxygen evolution activity in the presence of oxone. *Catal. Commun.* **11**, 1032–1035. (doi:10.1016/j.catcom.2010.04.016)

35 Ruttinger, W. & Dismukes, G. C. 1997 Synthetic water oxidation catalysts for artificial photosynthetic water oxidation. *Chem. Rev.* **97**, 1–24. (doi:10.1021/cr950201z)

36 Sproviero, E. M., Gascon, J. A., McEvoy, J. P., Brudvig, G. W. & Batista, V. S. 2008 Computational studies of the O₂-evolving complex of photosystem II and biomimetic oxomanganese complexes. *Coord. Chem. Rev.* **252**, 395–415. (doi:10.1016/j.ccr.2007.09.006)

37 Hou, H. J. M. 2011 Manganese-based materials inspired by photosynthesis for water-splitting. *Materials* **4**, 1693–1704. (doi:10.3390/ma4101693)

38 Hou, H. J. M. 2010 Structural and mechanistic aspects of Mn-oxo and Co-based compounds in water oxidation catalysis and potential application in solar fuel production. *J. Integr. Plant Biol.* **52**, 704–711. (doi:10.1111/j.1744-7909.2010.00974.x)

39 Liu, X. & Wang, F. 2012 Transition metal complexes that catalyze oxygen formation from water: 1979–2010. *Coord. Chem. Rev.* **256**, 1116–1136.

40 Najafpour, M. M., Nayeri, S. & Pashaei, B. 2011 Nano-size amorphous calcium–manganese oxide as an efficient and biomimetic water oxidizing catalyst for artificial photosynthesis: back to manganese. *Dalton Trans.* **40**, 9374–9378. (doi:10.1039/c1dt11048a)

41 Parmon, V. N., Elizarova, G. L. & Kim, T. V. 1982 Spinels as heterogeneous catalysts for oxidation of water to dioxygen by tris-bipyridyl complexes of iron(III) and ruthenium(III). *React. Kinet. Catal. Lett.* **21**, 195–197. (doi:10.1007/BF02070609)

42 Shafirovich, V. Y. & Shilov, A. E. 1979 Catalytic oxidation of water with the participation of manganese compounds in neutral and slightly acid media. *Kinet. Catal.* **20**, 1156–1162. [In Russian]

43 Morita, M., Iwakura, C. & Tamura, H. 1977 The anodic characteristics of manganese dioxide electrodes prepared by thermal decomposition of manganese nitrate. *Electrochim. Acta* **22**, 325–328. (doi:10.1016/0013-4686(77)85081-0)

44 Harriman, A., Pickering, I., Thomas, J. & Christensen, P. 1988 Metal oxides as heterogenous catalysts for oxygen evolution under photochemical condition. *J. Chem. Soc. Faraday* **84**, 2795–2801. (doi:10.1039/f19888402795)

45 Najafpour, M. M., Ehrenberg, T., Wiechen, M. & Kurz, P. 2010 Calcium manganese(III) oxides (CaMn₂O₄.xH₂O) as biomimetic oxygen-evolving catalysts. *Angew. Chem. Int. Ed.* **49**, 2233–2237. (doi:10.1002/anie.200906745)

46 Zaharieva, I., Najafpour, M. M., Wiechen, M., Haumann, M., Kurz, P. & Dau, H. 2011 Synthetic manganese–calcium oxides mimic the water-oxidizing complex of photosynthesis functionally and structurally. *Energy Environ. Sci.* **4**, 2400–2408. (doi:10.1039/c0ee00815j)

47 Najafpour, M. M. 2011 Calcium manganese oxides as structural and functional models for active site in oxygen evolving complex in photosystem II: lessons from simple models. *J. Photochem. Photobiol. B* **104**, 111–117. (doi:10.1016/j.jphotobiol.2010.12.009)

48 Najafpour, M. M. 2011 Amorphous manganese–calcium oxides as a possible evolutionary origin for the CaMn₄ cluster in photosystem II. *Orig. Life Evol. Biosph.* **41**, 237–247. (doi:10.1007/s11084-010-9224-z)

49 Jiao, F. & Frei, H. 2010 Nanostructure manganese oxide clusters supported on mesoporous silica as efficient oxygen-evolving catalysts. *Chem. Commun.* **46**, 2920–2922. (doi:10.1039/b921820c)

50 Najafpour, M. M., Pashaei, B. & Nayeri, S. 2012 Calcium manganese (IV) oxides: biomimetic and efficient catalysts for water oxidation. *Dalton Trans.* **41**, 4799–4805. (doi:10.1039/c2dt12189a)

51 Brimblecombe, R., Koo, A., Dismukes, G. C., Swiegers, G. F. & Spiccia, L. 2012 Solar-driven water oxidation by a bio-inspired manganese molecular catalyst. *J. Am. Chem. Soc.* **132**, 2892–2894. (doi:10.1021/ja910055a)

52 Najafpour, M. M., Amouzadeh Tabrizi, M., Haghighi, B. & Govindjee 2012 A manganese oxide with phenol groups as a promising structural model for water oxidizing complex in photosystem II: a 'golden fish'. *Dalton Trans.* **41**, 3906–3910. (doi:10.1039/c2dt11672c)

53 Hocking, R. K., Brimblecombe, R., Chang, L., Singh, A., Cheah, M. N., Glover, C., Casey, W. H. & Spiccia, L. 2011 Water-oxidation catalysis by manganese in a geochemical-like cycle. *Nat. Chem.* **3**, 461–465.

54 Najafpour, M. M. 2011 Self-assembled layered hybrid [Ru(bpy)₃]⁺² /manganese (III, IV) oxide: a new and efficient strategy for water oxidation. *Chem. Commun.* **47**, 11 724–11 726. (doi:10.1039/c1cc13895b)

55 Luneva, N. P., Shafirovich, V. Y. & Shilov, A. E. 1989 Catalytic and photocatalytic oxygen evolution from water in the presence of manganese complexes. *J. Mol. Catal.* **52**, 49–62. (doi:10.1016/0304-5102(89)80081-1)

56 Jiao, F. & Frei, H. 2010 Nanostructured cobalt and manganese oxide clusters as efficient water oxidation catalysts. *Energy Environ. Sci.* **3**, 1018–1027. (doi:10.1039/c002074e)

57 Navrotsky, A., Ma, C., Lilova, K. & Birkner, N. 2010 Nanophase transition metal oxides show large thermodynamically driven shifts in oxidation–reduction equilibria. *Science* **330**, 199–201. (doi:10.1126/science.1195875)

58 Jamnik, J. & Maier, J. 2003 Nanocrystallinity effects in lithium battery materials aspects of nano-ionics. *Phys. Chem. Chem. Phys.* **5**, 5215–5220. (doi:10.1039/b309130a)

59 Perez-Benito, J. F., Brillas, E. & Pouplana, R. 1989 Identification of a soluble form of colloidal manganese(IV). *Inorg. Chem.* **28**, 390–392. (doi:10.1021/ic00302a002)

60 Perez-Benito, J. F. & Arias, C. J. 1992 A kinetic study of the reaction between soluble (colloidal) manganese dioxide and formic acid. *J. Colloid Interface Sci.* **149**, 92–97. (doi:10.1016/0021-9797(92)90394-2)

61 Kumar, P. & Khan, Z. 2005 Oxidation of gum arabic by soluble colloidal MnO_2. *Carbohydr. Res.* **340**, 1365–1371. (doi:10.1016/j.carres.2005.02.017)

62 Najafpour, M. M. 2011 A soluble form of nano-sized colloidal manganese(IV) oxide as an efficient catalyst for water oxidation. *Dalton Trans.* **40**, 3805–3807. (doi:10.1039/c1dt00006c)

63 Najafpour, M. M., Pashaei, B. & Nayeri, S. 2012 Nano-sized layered aluminium or zinc-manganese oxides as efficient water oxidizing catalysts. *Dalton Trans.* **41**, 7134–7140. (doi:10.1039/c2dt30353a)

64 Boppana, V. B. R. & Jiao, F. 2011 Nanostructured MnO_2, an efficient and robust water oxidation catalyst. *Chem. Commun.* **47**, 8973–8975. (doi:10.1039/c1cc12258d)

65 Najafpour, M. M., Rahimi, F., Amini, M., Nayeri, S. & Bagherzadeh, M. 2012 A very simple method to synthesize nano-sized manganese oxide: an efficient catalyst for water oxidation and epoxidation of olefins. *Dalton Trans.* (doi:10.1039/C2DT30553D)

66 Amini, M., Najafpour, M. M., Nayeri, S., Pashaei, B. & Bagherzadeh, M. 2012 Nano-layered manganese oxides as low-cost, easily synthesized, environmentally friendly and efficient catalysts for epoxidation of olefins. *RSC Adv.* **2**, 3654–3657. (doi:10.1039/c2ra20297b)

67 Askarinejad, A., Bagherzadeh, M. & Morsali, A. 2010 Catalytic performance of Mn_3O_4 and Co_3O_4 nanocrystals prepared by sonochemical method in epoxidation of styrene and cyclooctene. *Appl. Surf. Sci.,* **256**, 6678–6682. (doi:10.1016/j.apsusc.2010.04.069)

68 Ghosh, R., Shen, X., Villegas, J. C., Ding, Y., Malinger, K. & Suib, S. L. 2006 Role of manganese oxide octahedral molecular sieves in styrene epoxidation. *J. Phys. Chem. B* **110**, 7592–7599. (doi:10.1021/jp056961n)

69 Shutova, T., Irrgang, K. D., Shubin, V., Klimov, V. V. & Renger, G. 1997 Analysis of pH-induced structural changes of the isolated extrinsic 33 kilodalton protein of photosystem II. *Biochem.* **36**, 6350–6358. (doi:10.1021/bi963115h)

70 Shutova, T., Nikitina, J., Deikus, G., Andersson, B., Klimov, V. V. & Samuelsson, G. 2005 Structural dynamics of the manganese-stabilizing protein effect of pH, calcium, and manganese. *Biochemistry* **44**, 15 182–15 192. (doi:10.1021/bi0512750)

71 Debus, R. J. 2008 Protein ligation of the photosynthetic oxygen-evolving center. *Coord. Chem. Rev.* **252**, 244–258. (doi:10.1016/j.ccr.2007.09.022)

72 Debus, R. J. 2001 Amino acid residues that modulate the properties of tyrosine Y_Z and the manganese cluster in the water oxidizing complex of photosystem II. *Biochim. Biophys. Acta* **1503**, 164–186. (doi:10.1016/S0005-2728(00)00221-8)

73 Yano, J., Walker, L. M., Strickler, M. A., Service, R. J., Yachandra, V. K. & Debus, R. J. 2011 Altered structure of the Mn_4Ca cluster in the oxygen-evolving complex of photosystem II by a histidine ligand mutation. *J. Biol. Chem.* **286**, 9257–9267. (doi:10.1074/jbc.M110.205740)

74 Stich, T. A., Yeagle, G. J., Service, R. J., Debus, R. J. & Britt, R. D. 2011 Ligation of D1-His332 and D1-Asp170 to the manganese cluster of photosystem II from *Synechocystis* assessed by multifrequency pulse EPR spectroscopy. *Biochemistry* **50**, 7390–7404. (doi:10.1021/bi2010703)

75 Najafpour, M. M., Sedigh, D. J., King'ondu, C. K. & Suib, S. L. Submitted. Nano manganese oxide-bovine serum albumin as a biomimetic catalyst for water oxidation.

76 Yu, S. 2007 Bio-inspired crystal growth by synthetic templates. *Top. Curr. Chem.* **271**, 79–118. (doi:10.1007/128_070)

77 Yang, L., Xing, R., Shen, Q., Jiang, K., Ye, F., Wang, J. & Ren, Q. 2006 Fabrication of protein-conjugated silver sulfide nanorods in the bovine serum albumin solution. *J. Phys. Chem. B*, **110**, 10 534–10 539. (doi:10.1021/jp055603h)

78 Qin, D., Ma, X., Yang, L., Zhang, L., Ma, Z. & Zhang, J. 2008 Biomimetic synthesis of HgS nanoparticles in the bovine serum albumin solution. *J. Nanopart. Res.* **10**, 559–566. (doi:10.1007/s11051-007-9284-9)

79 Iyer, A., Del-Pilar, J., King'ondu, C. K., Kissel, E., Garces, H. F., Huang, H., El-Sawy, A. M., Dutta, P. K. & Suib, S. L. 2012 Water oxidation catalysis using amorphous manganese oxides, octahedral molecular sieves (OMS-2), and octahedral layered (OL-1) manganese oxide structures. *Phys. Chem. C* **116**, 6474–6483. (doi:10.1021/jp2120737)

80 Mishra, A., Wernsdorfer, W., Abboud, K. A. & Christou, G. 2005 The first high oxidation state manganese–calcium cluster: relevance to the water oxidizing complex of photosynthesis. *Chem. Commun.* **2005**, 54–56. (doi:10.1039/b413680b)

81 Kanady, S., Tsui, E., Day, M. & Agapie, T. 2011 A synthetic model of the Mn_3Ca subsite of the oxygen-evolving complex in photosystem II. *Science* **333**, 733–736. (doi:10.1126/science.1206036)

82 Mukherjee, S. *et al.* 2012 Synthetic model of the asymmetric $[Mn_3CaO_4]$ cubane core of the oxygen-evolving complex of photosystem II. *Proc. Natl Acad. Sci. USA* **109**, 2257–2262. (doi:10.1073/pnas.1115290109)

83 Zhang, J., Ma, X., Guo, Y., Yang, L., Shen, Q., Wang, H. & Ma, Z. 2010 Size-controllable preparation of bovine serum albumin-conjugated. *Mater. Chem. Phys.* **119**, 112–118. (doi:10.1016/j.matchemphys.2009.08.027)

84 Najafpour, M. M., Moghaddam, N. A., Allakhverdiev, S. I. & Govindjee 2012 Biological water oxidation: lessons from nature. *Biochim. Biophys. Acta* **1817**, 1110–1121. (doi:10.1016/j.bbabio.2012.04.002)

85 Najafpour, M. M. & Govindjee 2011 Oxygen evolving complex in photosystem II: better than excellent. *Dalton Trans.* **40**, 9076–9084. (doi:10.1039/c1dt10746a)

86 Stranger, R. 2012 Why nature chose Mn for the water oxidase in photosystem II. *Dalton Trans.* **41**, 7179–7189. (doi:10.1039/C2DT30185G)

87 Armstrong, F. A. 2008 Why did nature choose manganese to make oxygen? *Phil. Trans. R. Soc. B* **363**, 1263–1270. (doi:10.1098/rstb.2007.2223)

88 Zulfugarov, I., Tovuu, A., Kim, J.-H. & Lee, C.-H. 2011 Detection of reactive oxygen species in higher plants. *J. Plant Biol.* **54**, 351–357.

89 Goh, C.-H., Ko, S.-M., Koh, S., Kim, Y.-J. & Bae, H.-J. 2012 Photosynthesis and environments: photoinhibition and repair mechanisms in plants. *J. Plant Biol.* **55**, 93–101.

90 Allakhverdiev, S. I. & Murata, N. 2004 Environmental stress inhibits the synthesis *de novo* of proteins involved in the photodamage-repair cycle of photosystem II in *Synechocystis* sp. PCC 6803. *Biochim. Biophys. Acta* **1657**, 23–32.

91 Murata, N., Allakhverdiev, S. I. & Nishiyama, Y. 2012 The mechanism of photoinhibition *in vivo*: Re-evaluation of the roles of catalase, α-tocopherol, non-photochemical quenching, and electron transport. *Biochim. Biophys. Acta* **1817**, 1127–1133.